Raman spectra could possibly alleviate this problem. Regardless, the bands at 159 (Ra) and 155 cm^{-1} (IR) are assigned to one of the two $\nu(HgI)_t$ modes associated with vibration of the two terminal, and also shortest, Hg–I bonds; the second IR- and Ra-active $\nu(HgI)_t$ modes are possibly accidentally coincident with the first pair. The bands at 131 and 111 cm^{-1} in the Raman spectrum and 133, 126, 103, and 99 cm^{-1} in the IR spectrum are assigned to $\nu(HgI)_b$ modes.[5,8,9,19,35,36] The wavenumber positions of all these modes lie in ranges consistent with more recent $\nu(HgI)_t$ and $\nu(HgI)_b$ assignments. It is worthwhile noting that these spectra, particularly at room temperature, could quite reasonably have been interpreted as those of a discrete dimeric molecule, therefore serving as a warning against the use of such data for structural prediction without first some very careful consideration.

Examination of the gross features of the $(TePh_2)HgBr_2$ spectra suggested a different structure to that of the iodo compound. The IR spectrum is particularly curious in the region 152–99 cm^{-1}, where a large number of bands can be assigned $\nu(HgBr)_b$, whereas the Raman spectrum in contrast is very simple with $\nu(HgBr)_b$ modes assigned at 158 and 127 cm^{-1}. The bands at 192 (Ra) and 194 cm^{-1} (IR) can confidently be assigned to $\nu(HgBr)$ modes associated with relatively short Hg–Br bond(s). No firm structural proposal can be made other than to tentatively predict a complicated bridging system.

Although hindered by the presence of internal modes of the $TePh_2$ ligand, $\nu(HgCl)$ modes have been assigned. The bands at 284 (IR) and 276 cm^{-1} (IR) almost certainly arise from $\nu(HgCl)$ modes associated with relatively short Hg–Cl bonds; the Ra band at 285 cm^{-1} no doubt has similar origins. Bands associated with $\nu(HgCl)_b$ are assigned at 230 and 134 cm^{-1} in the Raman spectrum and 227, 223, and 152 cm^{-1} in the IR spectrum. Unfortunately no firm structural proposal can be made.

Assignment of $\nu(HgTe)_t$ modes is difficult in view of their nonexistence in the literature and the absence of any obvious halogen-mass independent bands in the $(TePh_2)HgX_2$ spectra. Considering the effective mass of Te, when attached to two phenyl groups, and the position of $\nu(HgP)_t$ modes in $(PAr_3)HgX_2$ (X = Cl, Br, or I; Ar = C_6H_6[36] or o-$CH_3C_6H_5$[9]), which have been tentatively assigned in the 140-cm^{-1} region, one may speculate that the present $\nu(HgTe)_t$ modes lie below this value. Unfortunately, this is an especially complicated region in our spectra.

Acknowledgment. The authors thank the NSERC for financial assistance, Dr. I. W. Nowell (Sheffield City Polytechnic) and Dr. P. L. Goggin (University of Bristol) for infrared data, and Dr. F. Aubke (University of British Columbia) for use of Raman facilities.

Registry No. $(TePh_2)HgI_2$, 87509-57-7; $[(TePh_2)HgI_2]_4$, 87509-60-2; $(TePh_2)HgCl_2$, 87509-58-8; $(TePh_2)HgBr_2$, 87509-59-9.

Supplementary Material Available: Listings of anisotropic thermal parameters, hydrogen atom positions and temperature factors, bond distances and angles, and observed and calculated structure factors (24 pages). Ordering information is given on any current masthead page.

Contribution from the Departments of Chemistry and Physics, Monash University, Clayton, Victoria 3168, Australia, and Department of Physical and Inorganic Chemistry, University of Western Australia, Nedlands, Western Australia 6009, Australia

Structure, Magnetism, and Mössbauer Spectrum of the Five-Coordinate Complex Chlorobis(*N*-methylbenzothiohydroxamato)iron(III)

KEVIN J. BERRY,[1a] PAUL E. CLARK,[1b] KEITH S. MURRAY,*[1a] COLIN L. RASTON,[1c] and ALLAN H. WHITE[1c]

Received August 10, 1982

A detailed study of the structural, magnetic, ESR, and Mössbauer spectroscopic properties of a five-coordinate iron(III) thiohydroxamate complex has been made. The complex, chlorobis(*N*-methylbenzothiohydroxamato)iron(III), contains two trans bidentate {SO} donor groups and one Cl atom in each mononuclear unit and has bond distances Fe–Cl = 2.221 (2) Å, Fe–S = 2.389 (2) Å (average), and Fe–O = 1.946 (3) Å. This high-spin d^5 molecule has an overall ligand field strength provided by the $\{S_2O_2Cl\}$ donor set similar to that in related β-diketonate $\{O_4Cl\}$ complexes but weaker than that in intermediate-spin dithiocarbamate $\{S_4Cl\}$ species. Magnetic moment measurements between 4.2 and 300 K are generally consistent with the presence of large zero-field splitting effects although the decrease in μ_{Fe} at low temperatures is unusually rapid. In line with the low molecular symmetry and observation of g = 4.3 and 9.9 ESR spectral lines, a spin-Hamiltonian analysis, which includes rhombic and axial components, was carried out. The best-fit parameters were $D = 10 \pm 0.5$ cm^{-1} and $E = 3 \pm 0.5$ cm^{-1}. Weak antiferromagnetic coupling ($J = -0.1$ ■ 0.05 cm^{-1}) was also evident in the low-temperature susceptibility data and possibly occurs via a {Fe–Cl···Cl–Fe} superexchange pathway. Exchange coupling of this kind is common among other chloro–iron(III) chelate complexes containing a variety of oxygen, nitrogen, or sulfur donor groups. Zero-field Mössbauer spectra measured between 4.2 and 300 K on the present complex support the $S = {}^5/_2$ spin-state assignment and show unusual temperature-dependent area and peak height asymmetry. Applied magnetic field spectra at 4.2 K confirm the large and positive zero-field splitting of the $^6A_1$ ground state.

Introduction

Our recent studies of thiohydroxamate complexes of iron(III) afforded both bis- and tris-chelated species.[2,3] The properties of the tris chelate have been described in detail, and it is the purpose of this paper to report the results of a structural and electronic investigation on a representative bis chelate, chlorobis(*N*-methylbenzothiohydroxamato)iron(III) (labeled I). The compound has the formula [Fe(PhCSNMeO)$_2$Cl].

This five-coordinate complex is an example of a class of iron(III) compounds of general formulas [Fe(bidentate)$_2$X] and [Fe(tetradentate)X]. It is the first of such species containing the donor atoms {SO} within the chelate ligand although the tris complex [Fe(PhCSNMeO)$_3$] is well-known. Other donor sets that are known include {SS} in dithiocarbamates,[4] {OO} in β-diketonates,[5] {ON} in 8-hydroxy-

(1) (a) Department of Chemistry, Monash University. (b) Department of Physics, Monash University. Present address: Department of Applied Physics, Capricornia Institute of Advanced Education, Rockhampton, Queensland 4700, Australia. (c) University of Western Australia.
(2) Mitchell, A. J.; Murray, K. S.; Newman, P. J.; Clark, P. E. *Aust. J. Chem.* **1977**, *30*, 2439.
(3) Murray, K. S.; Newman, P. J.; Gatehouse, B. M.; Taylor, D. *Aust. J. Chem.* **1978**, *31*, 983.

0020-1669/83/1322-3928$01.50/0

quinolates[6] and salicylaldiminates,[7] and {NN} in porphyrins[8] and macrocycles.[9] The spin state of the metal ion is of particular interest since it can depend on such factors as the nature of the donor atoms, the chelate ligand, and the fifth ligand X and the symmetry of the ligand field. We have determined the structure of the present complex by X-ray crystallography and have investigated its magnetic susceptibility and Mössbauer spectra over a wide temperature range. We show that the compound (I) has pseudo-square-pyramidal geometry and displays high-spin magnetic behavior with large zero-field splitting and very weak antiferromagnetic coupling. Its properties are compared with those of related complexes containing oxygen, nitrogen, and sulfur donor atoms.

Experimental Section

Preparation of $[(PhCSNMeO)_2FeCl]$. Chlorobis(*N*-methylbenzothiohydroxamato)iron(III) (I) was prepared as described previously.[2] Anal. Calcd for $C_{16}H_{16}ClFeN_2O_2S_2$: C, 45.4; H, 3.8; N, 6.6; S, 15.1; Cl, 8.5. Found: C, 45.6; H, 4.0; N, 6.7; S, 15.2; Cl, 8.6. The crystalline sample used for the physical measurements appeared homogeneous under high magnification. All the crystals appeared to have identical morphology. Crystals suitable for X-ray studies were obtained by slow diffusion of low-boiling petroleum ether into the ethanolic preparative solution.

Magnetic Measurements. Magnetic susceptibility measurements over the temperature range 4.2–300 K were made on an Oxford Instruments Faraday balance that incorporated a superconducting solenoid and an automatic data-logging facility. The field strength was 10 kG and the field gradient 1000 G cm^{-1}. The temperatures were accurately calibrated by means of a gallium arsenide diode suspended in the sample position.[10]

Mössbauer-Effect Measurements. All Mössbauer measurements were made with a ^{57}Co in Rh source at room temperature, and the velocity scale and position of zero isomer shift were calibrated with an α-iron foil at room temperature. For the low-temperature data the specimen was immersed in liquid nitrogen or liquid helium respectively. Magnetic fields generated by a split pair of superconducting coils were applied perpendicular to the direction of propagation of the Mössbauer γ rays.

Electron Spin Resonance Spectra. A Varian E12 instrument was employed with an Oxford Instruments flow cryostat used for measurements at 4.3 K.

X-ray Structural Determination. The crystal data are as follows: $C_{16}H_{16}ClFeN_2O_2S_2$, M_r = 423.7, monoclinic, space group $P2_1/c$ (C_{2h}^5, No. 14), a = 9.052 (5) Å, b = 8.224 (7) Å, c = 25.888 (14) Å, β = 107.21 (4)°, V = 1841 (3) Å^3, d(obsd) = 1.52 (1) g cm^{-3}, d(calcd) = 1.53 g cm^{-3} (Z = 4), F(000) = 868; monochromatic Mo Kα radiation (λ = 0.710 69 Å, μ = 11.6 cm^{-1}); specimen size 0.17 × 0.42 × 0.20 mm.

The data were acquired with a Syntex $P\bar{1}$ four-circle diffractometer conventional $2\theta/\theta$ scan mode, a unique data set to $2\theta_{max}$ = 50° yielding 3216 independent reflections, 2480 of these with $I > 2\sigma(I)$ considered "observed" and used in the refinement after analytical absorption correction and solution by direct methods. Refinement was basically 9 × 9 block-diagonal least squares, but with $(x, y, z)_H$ refined in the block of the parent C and with the parameters of the $FeClO_2S_2$ molecular core refined as a single block. Thermal parameters used were anisotropic, except for U_H (isotropic), constrained at $1.25\bar{U}_{ii}$ (parent C). Residuals (R, R') were 0.038 and 0.042, reflection weights being $(\sigma^2(F_o) + 0.0003(F_o)^2)^{-1}$. Neutral-atom scattering factors were used; all atoms except H were corrected for anomalous dispersion ($\Delta f'$, $\Delta f''$).[11] Computations employed the X-RAY 76 program system[12] on

Table I. Non-Hydrogen Atom Fractional Cell Coordinates

atom	x/a	y/b	z/c
Fe	0.7034 (1)	0.1858 (1)	0.1212 (1)
Cl	0.6537 (1)	0.4072 (1)	0.0698 (1)
S(A)	0.9574 (1)	0.0894 (1)	0.1276 (1)
S(B)	0.4740 (1)	0.1399 (1)	0.1467 (1)
O(A)	0.6444 (2)	0.0065 (3)	0.0702 (1)
O(B)	0.7825 (3)	0.2533 (3)	0.1964 (1)
C(A)	0.8987 (3)	−0.0651 (4)	0.0818 (1)
C(A1)	1.0165 (4)	−0.1776 (4)	0.0726 (1)
C(A2)	1.1465 (5)	−0.1174 (5)	0.0616 (2)
C(A3)	1.2599 (5)	−0.2211 (6)	0.0556 (2)
C(A4)	1.2457 (5)	−0.3864 (6)	0.0610 (2)
C(A5)	1.1190 (5)	−0.4462 (5)	0.0731 (2)
C(A6)	1.0033 (4)	−0.3439 (5)	0.0786 (2)
N(A)	0.7511 (3)	−0.0859 (3)	0.0573 (1)
C(A7)	0.6808 (5)	−0.1988 (5)	0.0130 (2)
C(B)	0.5400 (4)	0.2321 (4)	0.2081 (1)
C(B1)	0.4324 (4)	0.2523 (4)	0.2414 (1)
C(B2)	0.2898 (4)	0.3262 (5)	0.2185 (2)
C(B3)	0.1828 (5)	0.3361 (6)	0.2473 (2)
C(B4)	0.2188 (6)	0.2729 (6)	0.2985 (2)
C(B5)	0.3592 (6)	0.1993 (6)	0.3215 (2)
C(B6)	0.4655 (5)	0.1900 (5)	0.2933 (2)
N(B)	0.6843 (3)	0.2786 (3)	0.2261 (1)
C(B7)	0.7610 (5)	0.3606 (6)	0.2770 (2)

Table II. Non-Hydrogen Molecular Geometry[a]

	Distances (Å)
Fe-Cl	2.221 (2)
Fe-S	2.391 (2), 2.387 (2); 2.4445 (5); 2.445 (14)
Fe-O	1.946 (3), 1.946 (3); 2.0098 (11); 1.990 (6)
S···O	2.865 (3), 2.863 (3); 2.910 (1); 2.87 (2)
S-C	1.712 (3), 1.703 (3); 1.681 (2); 1.703 (3)
O-N	1.346 (4), 1.353 (4); 1.342 (2); 1.348 (4)
C-N	1.310 (4), 1.308 (4); 1.295 (2); 1.307 (2)
N-C(7)	1.468 (5), 1.459 (5); 1.458 (3); 1.468 (2)
C-C(1)	1.484 (5), 1.488 (6)
C(1)-C(2)	1.381 (6), 1.391 (5)
C(2)-C(3)	1.379 (7), 1.389 (7)
C(3)-C(4)	1.376 (7), 1.369 (7)
C(4)-C(5)	1.367 (7), 1.374 (7)
C(5)-C(6)	1.384 (6), 1.370 (8)
C(6)-C(1)	1.385 (5), 1.386 (5)
	Angles (deg)[b]
Cl-Fe-S	109.51 (5), 104.85 (5)
Cl-Fe-O	104.39 (9), 108.34 (10)
S-Fe-O	82.02 (8), 82.02 (9); 80.94 (3); 80.0 (2)
Fe-S-C	95.9 (1), 95.4 (1); 94.41 (7); 95.7 (10)
Fe-O-N	121.5 (2), 120.2 (2); 118.63 (8); 120.8 (8)
S-C-C(1)(H)	119.0 (2), 118.8 (2); (124.1 (15)); 119.2 (2)
S-C-N	119.7 (3), 120.0 (3); 122.4 (2); 120.2 (5)
(H)C(1)-C-N	121.3 (3), 121.2 (3); (112.9 (15)); 120.7 (6)
O-N-C(7)	112.0 (3), 111.5 (3); 114.1 (1); 111.5 (5)
O-N-C	120.7 (3), 120.5 (3); 121.5 (2); 120.6 (7)
C(7)-N-C	127.3 (3), 128.0 (3); 124.4 (2); 127.5 (5)
C-C(1)-C(2)	120.4 (3), 119.1 (3)
C-C(1)-C(6)	120.5 (3), 122.0 (3)
C(2)-C(1)-C(6)	118.9 (4), 118.8 (4)
C(1)-C(2)-C(3)	120.7 (4), 120.2 (4)
C(2)-C(3)-C(4)	120.3 (5), 119.5 (4)
C(3)-C(4)-C(5)	119.3 (5), 120.8 (5)
C(4)-C(5)-C(6)	121.1 (4), 119.9 (4)
C(5)-C(6)-C(1)	119.7 (4), 120.8 (4)

[a] The first two values in each entry correspond to sections A and B of the molecule, respectively, the third is the value for the parameters found in $[(HCSNMeO)_3Fe]$, and the fourth is the mean found in $[(PhCSNMeO)_3Fe]$. [b] Interligand core angles: O(A)-Fe-O(B), 147.26 (11)°; S(A)-Fe-S(B), 145.63 (5)°; O(A)-Fe-S(B), 88.94 (8)°; O(B)-Fe-S(A), 87.89 (8)°.

(4) Martin, R. L.; White, A. H. *Inorg. Chem.* **1967**, *6*, 712.
(5) Cox, M.; Fitzsimmons, B. W.; Smith, A. W.; Larkworthy, L. F.; Rogers, K. A. *J. Chem. Soc. A* **1971**, 2158.
(6) Cunningham, D.; Frazer, M. J.; Qureshi, A. H.; Taylor, F. B.; Dale, B. W. *J. Chem. Soc., Dalton Trans.* **1972**, 1090.
(7) Van den Bergen, A.; Murray, K. S.; Rehak, N.; West, B. O. *Aust. J. Chem.* **1968**, *21*, 1505. Davies, J. E.; Gatehouse, B. M. *J. Chem. Soc. D* **1970**, 1166.
(8) Hatano, K.; Scheidt, W. R. *Inorg. Chem.* **1979**, *18*, 877 and references therein.
(9) Koch, T. H.; Holm, R. H.; Frankel, R. B. *J. Am. Chem. Soc.* **1975**, *97*, 6714.
(10) Mackey, D. J.; Evans, S. V.; Martin, R. L. *J. Chem. Soc., Dalton Trans.* **1976**, 1515.
(11) "International Tables for X-ray Crystallography"; Ibers, J. A., Hamilton, W. C., Eds.; Kynoch Press: Birmingham, England, 1974; Vol. IV.

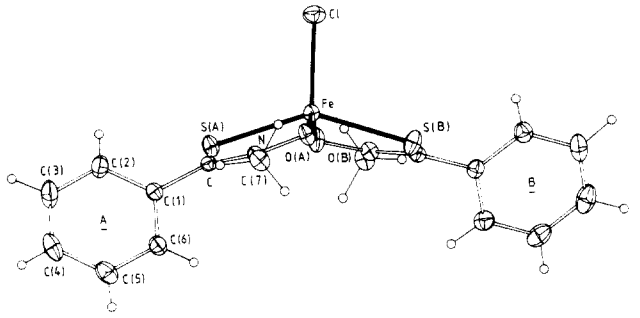

Figure 1. Molecular projection of $[Fe(PhCSNMeO)_2Cl]$.

Table III. Comparative Molecular Core Geometries[a]

	i	ii	iii
Fe–Cl	2.28_1	2.22_1	2.21_8
Fe–S	2.28_7	2.38_9	
Fe–O		1.94_6	1.9_5
X···X(Y)[b]	2.80_6	2.86_4	
Cl–Fe–S	$106._5$[d]	$107._2$	
Cl–Fe–O		$106._4$[d]	
S–Fe–S(O)[b]	$75._7$	82.0_2	
S–Fe–S(O)[c] (cis)	$95._1$	$88._4$	
S–Fe–S[c] (trans)	$147._0$[d]	$145._6$	
O–Fe–O		$147._3$	

[a] Comparative geometries are given for (i) the $FeClX_2Y_2$ molecular core in $[(R_2NCS_2)_2FeCl]$ (the values given are for the recently determined example where R is isopropyl, these being more precise than those reported earlier for R = ethyl), (ii) the present compound, and (iii) $[(C_5H_7O_2)_2FeCl]$. Distances (Å) and angles (deg) are mean values for the compound given. [b] Intraligand. [c] Interligand. [d] Mean of widely differing values.

a CYBER 73 computer. Atom numbering within the ligands A and B is as shown in Figure 1, hydrogen atoms being numbered according to the parent carbon and prefixed 1, 2, 3 in the case of the methyl groups.

The following results for $[(PhCSNMeO)_2FeCl]$ are tabulated: non-hydrogen atom fractional cell coordinates (Table I), non-hydrogen molecular geometry (Table II), comparative molecular core geometries (Table III). The following are available as supplementary material: least-squares planes (Table V), non-hydrogen atom anisotropic thermal parameters (Table VI), atomic fractional cell and isotropic thermal parameters (hydrogen atoms) (Table VII), hydrogen atom geometries (Table VIII), structure factor amplitudes (Table IX). The structure of the molecule is shown in Figure 1. The unit cell contents projected down *b* are shown in Figure 7 (supplementary data).

Results and Discussion

Description of the Structure. The unit cell contents comprise discrete molecules of the complex $[(PhCSNMeO)_2FeCl]$, the asymmetric unit of the structure being an individual molecule. The only intermolecular interaction shorter than the usual van der Waals contact distances appears to be Cl···H(A6) (x, 1 + y, z), 2.90 (4) Å.

Within the molecule, the environment of the iron atom is five-coordinate; in complexes such as the related $[(R_2NCS_2)_2FeX]$[13] it is common and convenient to describe the iron environment as pseudo square pyramidal, the halide atom being at the apex of the pyramid. In the present complex, the ligand is unsymmetrically bidentate, giving scope for isomerism, and in the above convention we find that the two sulfur atoms are trans rather than cis in the pyramid base and, accordingly, the maximum point symmetry of the $FeLX_4$ system is lowered from C_{2v} to C_2. In the present example, the actual symmetry of the system is even lower as a rather surprising disparity is observed between the angles subtended at the iron atom by the two interligand ClSO triangular faces, the ClS(B)O(A) face being more compact than the ClS(A)-O(B) face and the respective S–Fe–Cl and S–Fe–O angle pairs differing from each other by some 4° (approximately) (Table II). In view of the generally good agreement among the other interligand core angles, it appears that this distortion may be a consequence of displacement of the apical chlorine atom toward O(A) and S(B), probably in turn a result of the above hydrogen-bonding interaction. However, the gross disparity in the iron atom deviations from the two conjugated ligand planes (supplementary data) shows that this description is an oversimplification (Wide discrepancies of this type have already been reported elsewhere for related compounds, e.g. $[(i\text{-}Pr_2NCS_2)_2FeCl]\cdot CHCl_3$.[13])

Although the geometry about the iron atom does not conform closely to any idealized symmetry in terms of its angular geometry, there is generally good agreement throughout the remainder of the molecular dimensions for pairs of equivalent parameters (Table II). Comparison of the dimensions of the present $ClFeS_2O_2$ system is made with those for other known examples of $ClFeS_4$ and $ClFeO_4$ systems in Table III. Although the information available on $[(acac)_2FeCl]$[5,14] is limited, both Fe–O and Fe–Cl distances are in good agreement with those of the present compound, while Fe–Cl and Fe–S of the present compound differ considerably from those of the $[(R_2NCS_2)_2FeCl]$ systems so far reported. (The ring size formed by the chelate ligands in the present example, being five-membered, lies intermediate between those of the other two complexes.)

It is of interest to also compare the ligand dimensions in the present compound with those of the parent tris complex[15] and of tris(*N*-methylformothiohydroxamato)iron(III),[3,16] the two systems differing in metal–ligand distances that are longer in the tris complex (Table II) and in the attachment of the phenyl group. Although there are generally minor differences in most dimensions, chiefly attributable to the change in metal–ligand distance, a larger change is found in the angular geometry about the C–N(ring) bond; the general trend suggests that the exocyclic angles in the present compound and the tris complex contained by the phenyl and methyl groups are enlarged relative to those in the methyl complex, probably as a consequence of phenyl/methyl group repulsion. In the present compound (Table V), the phenyl ring in each ligand makes an angle of 54° with the FeSCNO ring plane and inspection of phenyl/methyl "contacts" H(A6)···H(3A7), 2.61 (5) Å, and H(B6)···H(3B7), 2.47 (6) Å, suggests these as the probable origin of this interaction.

Magnetic Properties. The average magnetic moments of I are plotted as a function of temperature in Figure 2, and the detailed χ_{Fe} vs. T data are given in Table X (supplementary data). Above ca. 70 K the moment has the value 5.81 μ_B and is independent of temperature. Below 70 K it begins to decrease quite rapidly, reaching a value of 3.87 μ_B at 4.2 K. This behavior is generally reminiscent of a $^6A_1$ state having considerable zero-field splitting as is observed in tetragonally distorted species of the type [Fe(porphyrin)Cl][17,18] or trigonally distorted species such as [Fe(pyrrolidyl-dtc)$_3$].[19] However, there are differences in detail. The μ_{Fe} value at 4.2 K is significantly lower than usual while μ_{Fe} above 70 K is also

(12) "The X-Ray System—Version of March 1976", Technical Report TR-446; Stewart, J. M., Ed.; Computer Science Center, University of Maryland: College Park, MD, 1976.
(13) Mitra, S.; Figgis, B. N.; Raston, C. L.; Skelton, B. W.; White, A. H. *J. Chem. Soc., Dalton Trans.* **1979**, 753.
(14) Lindley, P. F.; Smith, A. W. *J. Chem. Soc. D* **1970**, 1355.
(15) Freyberg, D. P.; Abu-Dari, K.; Raymond, K. N. *Inorg. Chem.* **1979**, *18*, 3037.
(16) Murray, K. S.; Newman, P. J.; Taylor, D. *J. Am. Chem. Soc.* **1978**, *100*, 2251.
(17) Maricondi, C.; Swift, W.; Straub, D. K. *J. Am. Chem. Soc.* **1969**, *91*, 5205.
(18) Marathe, V. R.; Mitra, S. *Chem. Phys. Lett.* **1973**, *19*, 140.
(19) Marathe, V. R.; Mitra, S. *Chem. Phys. Lett.* **1973**, *21*, 62.

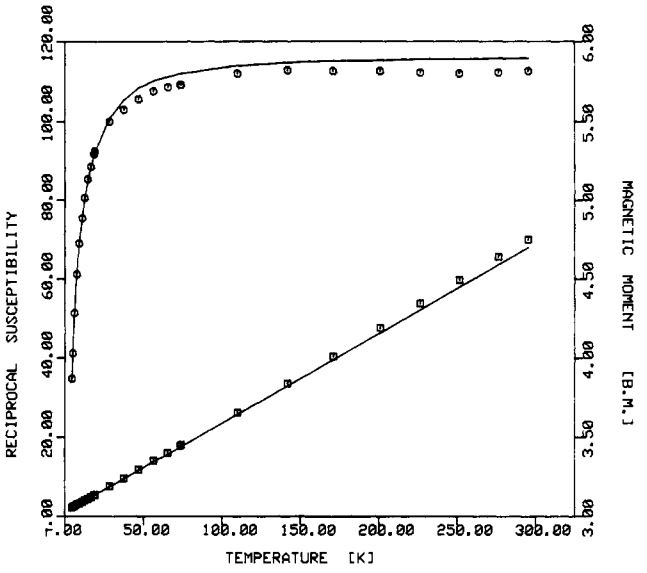

Figure 2. Magnetic moment per molecule (○) and reciprocal susceptibility (□) vs. temperature curves for [Fe(PhCSNMeO)$_2$Cl]. The solid line represents the best fit of the data. The parameters are given in the text.

reduced a little from the spin-only value of 5.92 μ_B.

A preliminary analysis of the magnetic data using a simple axial spin Hamiltonian of the $D\hat{S}_z^2$ type did not allow a good fit at all temperatures. Since the dependence of μ_{Fe} on T is rather atypical, it was only possible to improve the fit by having different D values at different temperatures, a most implausible situation. The next step was to use an abbreviated quadratic spin Hamiltonian with a rhombic term present:

$$\mathcal{H} = D\left[\hat{S}_z^2 - S\frac{S+1}{3}\right] + E(\hat{S}_x^2 - \hat{S}_y^2) + g\beta\hat{H}\cdot\hat{S}$$

This is more compatible with the low symmetry of the present compound (C_2) and in line with the ESR results. The magnetic moments and g values in the principal directions were calculated by computer diagonalization of the matrix obtained from the operation of the above Hamiltonian on the $^6A_1$ basis function set. The thermodynamic expression for susceptibility was employed, which is more appropriate to d^5 systems than is Van Vleck's equation.[18] The Mössbauer and ESR results, described below, show that D is positive and the ratio E/D is probably less than or equal to the "rhombic" condition, $^1/_3$.

μ_{Fe} values as a function of temperature were calculated for a wide range of D values, both positive and negative, and for various E/D ratios. Some typical plots are shown in Figure 3a, in which D is constant and E is increased from zero. It can be seen that the chief differences are at low temperatures; as E increases, the rate of decrease in μ_{Fe} becomes less rapid while the final base value is lowered. While inclusion of an E term improves the fit of the present data compared to that of the simple axial model, it was not possible to get a perfect fit. Neither the reduction of μ_{Fe} to 5.81 μ_B in the high-temperature region nor the rapid decrease in μ_{Fe} at low temperatures could be exactly reproduced.

There are three likely reasons for this lack of agreement. They are (i) the presence of some paramagnetic impurity that affects the low-temperature region in particular, (ii) the omission of fourth-order ligand field terms from the spin Hamiltonian, and (iii) the presence of weak magnetic exchange coupling between neighboring Fe(III) centers in the crystal lattice.

Dealing first with point i, we note from the ESR discussion (below) that the bulk sample appears to contain about 1% of the corresponding Cu(II) chelate, which is not surprising in view of the strong binding preference for copper displayed by thiohydroxamate ligands[20] and the tendency for commercial iron salts to contain trace quantities of other transition ions. Other than this, the crystalline samples used for the susceptibility and ESR studies appear homogeneous under high magnification while the microanalytical figures are very good (see Experimental Section). The presence of 1% CuL_2 has very little effect on the calculated magnetic moments at any temperatures and certainly cannot explain the shape of the observed μ_{Fe}/T curve. Significant quantities of an impurity displaying a rapidly *decreasing* moment at lower temperatures would be required to fit the curve, and there is no evidence for any such species being present. The theoretical background to point ii has been dealt with recently by a number of authors and applied to calculations of magnetic susceptibilities,[18,19] ESR g values,[21-23] and Mössbauer line shapes[21] of various bacterial Fe(III) siderophores and Fe(III) chelate complexes. Marathe and Mitra have recently fitted the low-temperature μ/T data for tetragonally distorted [Fe(protoporphyrin IX)Cl] and trigonally distorted [Fe(pyrrolidyl-dtc)$_3$] by including fourth-order ligand field terms but omitting rhombic terms.[18,19] In both cases the published data showed deviations from simple axial theory in a manner related to, but not identical with, that of I. We have explored Marathe and Mitra's approach, although neither axial nor trigonal symmetry is strictly applicable to the present molecular symmetry or to the ESR results (vide infra). It is possible by so doing to improve the fit of the magnetic data compared to that of DS_z^2 theory, but a perfect fit at all temperatures was not possible for physically reasonable parameter values. Subsequent studies on both the pyrrolidinecarbodithioate[24,25] and porphyrin Fe(III) complexes[26,27] have in fact revealed the presence of weak exchange coupling between neighboring Fe(III) centers. This brings us to alternative iii, which is the preferred description for the present results.

An exchange term of the form of a Heisenberg linear chain was incorporated into the quadratic Hamiltonian given above. After a thorough exploration of combinations of D, E, and J, it was found that a good fit of the data could be obtained in the sensitive region below ca. 70 K while small deviations were apparent at high temperatures (Figure 2) for the parameter values

$$D = 10 \pm 0.5 \text{ cm}^{-1} \qquad E = 3 \pm 0.5 \text{ cm}^{-1}$$
$$J = -0.1 \pm 0.05 \text{ cm}^{-1}$$

The calculations were particularly sensitive to small changes in J (Figure 3b). A study of the susceptibilities at temperatures below 4.2 K would be helpful in confirming the magnitude of this weak antiferromagnetic coupling. It is interesting to note the occurrence of weak exchange coupling in many five-coordinate Fe^{III} complexes related to complex I. Weak coupling has now been identified in polycrystalline samples of, for example, [Fe(acac)$_2$Cl],[5,28] [Fe(Et$_2$dtc)$_2$Cl],[29] [Fe(TPP)Cl], [Fe(OEP)Cl], and hemin[26,27] by means of magnetic,

(20) Becher, J.; Brockway, D. J.; Murray, K. S.; Newman, P. J.; Toftlund, H. *Inorg. Chem.* **1982**, *21*, 1791.
(21) Oosterhuis, W. T. *Struct. Bonding (Berlin)* **1974**, *20*, 59.
(22) Pilbrow, J. R. *J. Magn. Reson.* **1978**, *31*, 479.
(23) Sato, M.; Rispin, A. S.; Kon, H. *Chem. Phys.* **1976**, *18*, 211.
(24) Cukauskas, E. J.; Deaver, B. S.; Sinn, E. *J. Chem. Soc., Chem. Commun.* **1974**, 698.
(25) Hall, G. R.; Hendrickson, D. N. *Inorg. Chem.* **1976**, *15*, 607.
(26) Mitra, S. In "Physical Bioinorganic Chemistry—Iron Porphyrins, Part, 1"; Lever, A. B. P., Gray, H. B., Eds.; Addison-Wesley: Reading, MA, 1983; pp 1-42.
(27) Ernst, J.; Subramanian, J.; Fuhrhop, J. R. *Z. Naturforsch., A* **1977**, *32A*, 1129.
(28) Fitzsimmons, B. W.; Johnson, C. E. *Chem. Phys. Lett.* **1970**, *6*, 267.
(29) Wickman, H. H.; Trozzolo, A. H. *Symp. Faraday Soc.* **1967**, *No. 1*, 21.

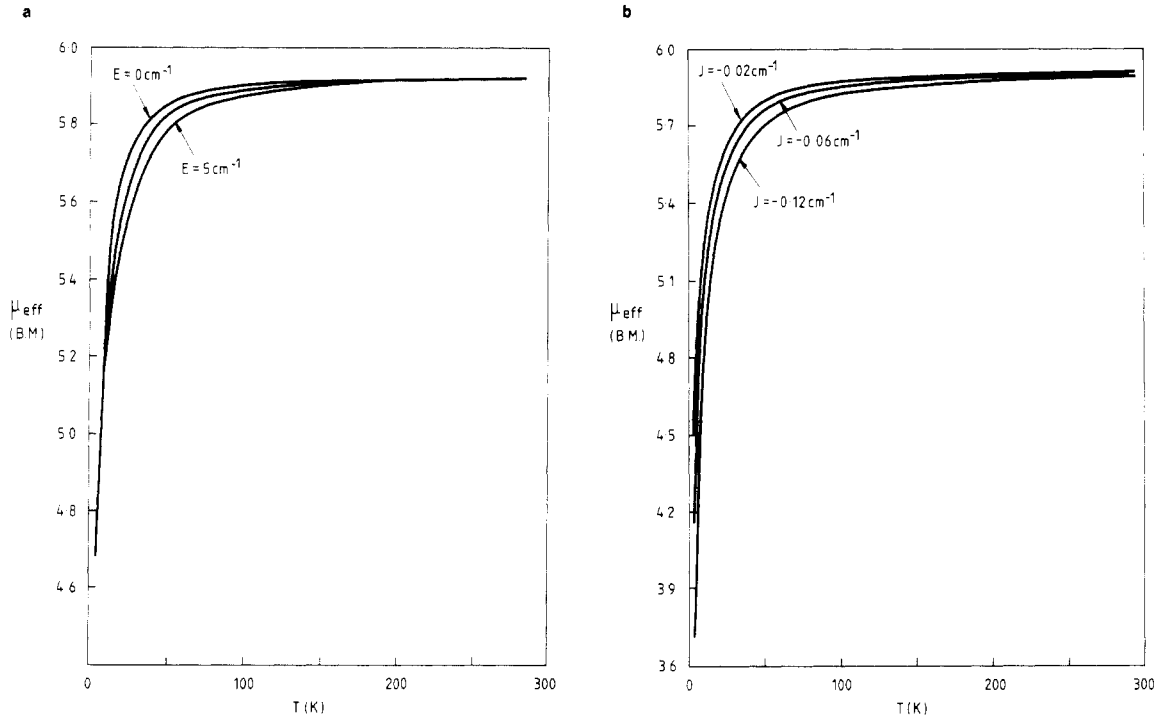

Figure 3. (a) Calculated temperature dependence of μ_{eff} for high-spin d^5 with $D = 10$ cm^{-1} and $E = 0$, 3, and 5 cm^{-1}. (b) Calculated temperature dependence of μ_{eff} for high-spin d^5 with $D = 10$ cm^{-1}, $E = 3$ cm^{-1}, and $J = -0.02$, -0.06, and -0.12 cm^{-1}.

ESR, and Mössbauer studies. In these examples, an in I, it is not obvious always from the crystal structure which are in the probable pathways for superexchange between widely spaced Fe^{III} centers. Since the chelate ligands are disparate in nature, it is tempting is suggest that the Fe^{III}–Cl moiety is the key feature, but this would not explain the similar weak coupling detected in [Fe(pyrrolidyl-dtc)$_3$]. In the lattice of the present complex a Cl···Cl $(1 - x, 1 - y, 1 - z)$ distance of 4.145 (3) Å provides the most likely, albeit unusual, exchange pathway. A similar interaction has been proposed in [Fe(T-PP)Cl].[26]

Electron Spin Resonance Spectra. X-Band ESR spectra of polycrystalline and $CHCl_3$/acetonitrile samples of I recorded at 4.2 K are shown in Figure 4. The spectrum of the neat solid is very broad and poorly resolved due to exchange broadening. It shows a major inflection at $g = 4.2$ and weaker features at $g =$ ca. 2.84, 2.04, and 1.94. The latter is sharper than the others and may well be due to a trace impurity. Unfortunately, the information to be gained from the solid spectrum is limited and measurements are desirable on a diluted sample (e.g. into a Co(III) or Al(III) analogue). In the absence of such data it is nevertheless possible to conclude that the ligand field giving rise to this spectrum is rhombic to some degree. On dissolution in $CHCl_3$/acetonitrile or $CHCl_3$/toluene solvent mixtures, intensly red solutions are obtained ($\lambda_{max} = 600$ nm) that, on freezing to 4.2 K, yield the spectrum shown in Figure 4b. A strong isotropic $g = 4.3$ line is observed, with peak to peak line width of 60 G, together with a weak inflection at $g =$ ca. 9.9. The weak multiplet at $g = 2$ is identified as being due to trace amounts of the Cu(II) chelate on account of its line shape.[20] Comparison of its area to those of the Fe(III) lines indicates a concentration of ca. 1%. The positions and relative intensities of the iron lines in the frozen-glass spectra are typical of a rhombically distorted environment in which D is positive.

Calculation of g values from the best-fit zero-field parameters obtained in the magnetic study gave values of 4.1–4.5 (from middle Kramers levels) and ca. 9.6 (from ground Kramers doublet), the latter predicted to be stronger as the temperature is lowered. The agreement with the observed g values in the frozen-glass spectrum, though satisfying, may be somewhat fortuitous since these calculated values are derived from susceptibility data from the solid, the corresponding ESR spectrum of which is poorly resolved.

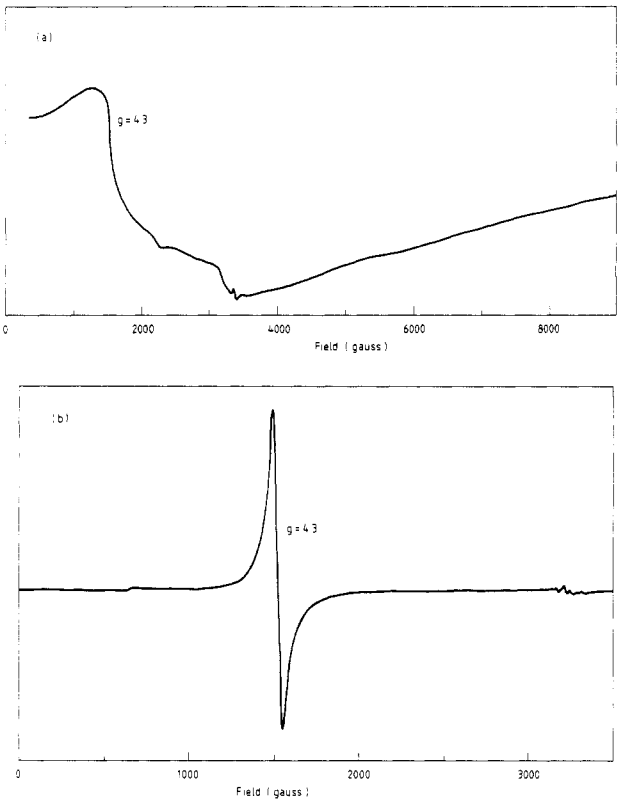

Figure 4. (a) X-Band ESR spectrum at 4.2 K of polycrystalline [Fe(PhCSNMeO)$_2$Cl]. (b) X-Band ESR spectrum at 4.2 K of [Fe(PhCSNMeO)$_2$Cl] in chloroform/acetonitrile glass.

Mössbauer-Effect Spectra. Mössbauer spectra for a polycrystalline sample of compound I at temperatures of 300, 77, and 4.2 K in zero applied magnetic field are shown in Figure

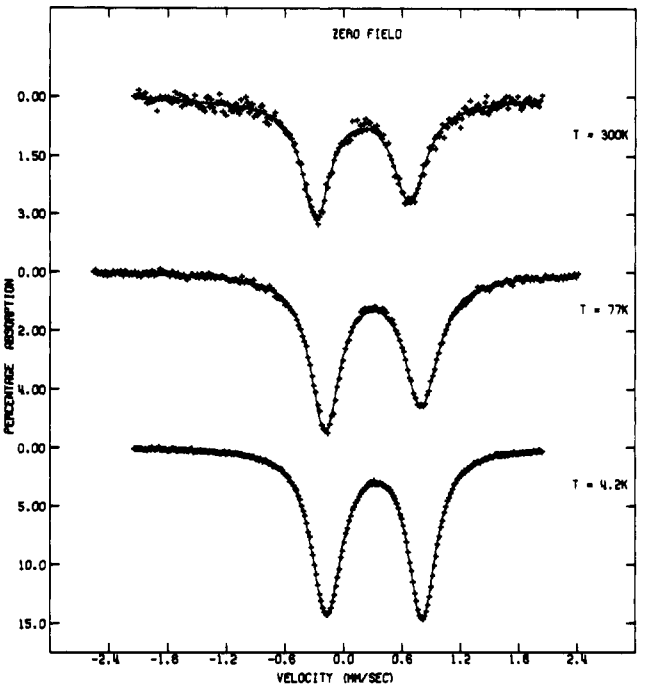

Figure 5. Mössbauer spectra of [Fe(PhCSNMeO)$_2$Cl] in zero applied field at 300, 77, and 4.2 K.

Table IV. Zero-Field Mössbauer Parameters of [(PhCSNMeO)$_2$FeCl] (I)

temp, K	δ (±0.01),[a] mm s^{-1}	ΔE (±0.01),[b] mm s^{-1}	full width (±0.01), mm s^{-1} line 1	full width (±0.01), mm s^{-1} line 2	area ratio (±0.005) line 1/ line 2
300	+0.32	0.96	0.34	0.38	1.028
77	+0.42	0.98	0.36	0.41	1.058
4.2	+0.43	0.98	0.38	0.34	1.096

[a] Isomer shift. [b] Quadrupole splitting.

5. Each spectrum consists of a single quadrupole-split doublet, and the values of the isomer shift and quadrupole splitting obtained by computer fitting two unconstrained Lorentzian lines to the spectra are given in Table IV. The quadrupole splitting is essentially independent of temperature, and the increase in isomer shift with decreasing temperature is attributable entirely to the second-order Doppler shift; these parameters lie in the range expected for $S = {}^5/_2$ iron(III), with the quadrupole splitting within the limits observed for similar chloro–iron(III) species such as [Fe(acac)$_2$Cl][5] and [Fe(porphyrin)Cl].[30]

Although the 4.2 K spectrum appears almost symmetric, the two lines have a difference in area of nearly 10%, with this difference decreasing as the temperature is raised. This somewhat unusual behavior resembles the Goldanskii–Karyagin effect observed in [Fe(salen)$_2$Cl],[31] but in the latter case the asymmetry increases as the temperature is raised. A combination of Goldanskii–Karyagin effect and slight orientation of the sample crystallites may explain the present observations. The asymmetry in peak intensity that develops at higher temperatures, while very much less marked than occurs in, for example [Fe(OEP)Cl],[30,32] is typical of high-spin ferric compounds that have a large, positive zero-field splitting parameter, D. It has been interpreted by Blume in terms of a temperature-dependent spin–spin relaxation time.[33] At low temperatures only the rapidly relaxing $S_z = |\pm{}^1/_2\rangle$ is occupied and an unbroadened spectrum is observed; at higher temperature the $S_z = |\pm{}^3/_2\rangle$ and $S_z = |\pm{}^5/_2\rangle$ states are also occupied and their longer relaxation times lead to preferential broadening of one line of the quadrupole doublet. The fact that it is the higher energy line that broadens first implies that the sign of V_{zz} (the principal component of the electric field gradient tensor) is positive, provided that V_{zz} and the z axis of the magnetic hyperfine field are parallel. Single-crystal studies would be required to prove the latter requirement. V_{zz} is also positive in various [Fe(porphyrin)Cl][30,32] complexes and in [Fe(acac)$_2$Cl].[5,28]

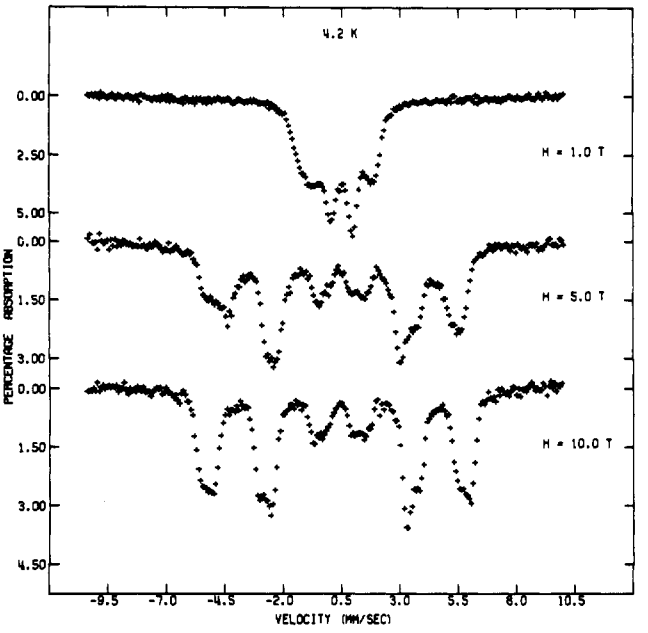

Figure 6. Mössbauer spectra of [Fe(PhCSNMeO)$_2$Cl] at 4.2 K in transverse applied fields of 1.0, 5.0, and 10.0 T.

Mössbauer spectra of I at 4.2 K and in transverse applied magnetic fields of 1.0, 5.0, and 10.0 T are shown in Figure 6. For small values of $H_{applied}$ poorly defined broad wings appear in addition to the sharp unperturbed doublet. At higher fields the spectrum develops a resolved hyperfine pattern of six lines, but with each line displaying some fine structure. These results can be understood in terms of a crystal field parameter D that is large and positive (i.e. $D >> 4.2$ K). In this case only the $S_z = |\pm{}^1/_2\rangle$ ground state is appreciably populated at 4.2 K. The main feature of the Mössbauer spectrum should be a magnetic hyperfine field of magnitude

$$H_{eff} = H_{applied} + \frac{\langle S_\perp \rangle}{S} H_{hf}$$

where H_{eff} is the effective field seen by an iron nucleus, H_{hf} is the saturation hyperfine field, and $\langle S_\perp \rangle / S$ is the perpendicular magnetization expressed as a fraction of its saturation value.[30] H_{hf} is a negative quantity (i.e. oppositely directed to the applied field). The maximum effective hyperfine fields determined by inspection of the Mössbauer spectra in Figure 6 are 9.7, 34.9, and 36.1 T in applied fields of 1.0, 5.0, and 10.0 T, respectively. It is possible to fit these H_{eff} values to the Brillouin function appropriate to a large tetragonal distortion (i.e. no field-induced mixing of levels) with a value of H_{hf} of 47.5 T, which is comparable to values obtained for various iron(III) porphyrins.[30] While this further confirms the positive sign for D, it remains an approximation for the

(30) Sams, J. R.; Tsin, T. B. In "The Porphyrins"; Dolphin, D., Ed.; Academic Press: New York, 1979; Vol. IV, Chapter 9.
(31) Buckley, A. N.; Herbert, I. R.; Rumbold, B. D.; Wilson, G. V. H.; Murray, K. S. *J. Phys. Chem. Solids* **1970**, *31*, 1423.
(32) Dolphin, D. H.; Sams, J. R.; Tsin, T. B.; Wong, K. L. *J. Am. Chem. Soc.* **1978**, *100*, 1711. Fitzsimmons, B. W.; Sams, J. R. *Chem. Phys. Lett.* **1976**, *38*, 588.
(33) Blume, M. *Phys. Rev. Lett.* **1967**, *18*, 305.

rhombically distorted situation. Finally, it is noteworthy that the small negative J value deduced from the susceptibility data does not markedly attenuate the Mössbauer hyperfine splitting, as it does in more strongly antiferromagnetically coupled molecules of the types $[Fe(acac)_2Cl]$[5,28] and $[Fe(salen)_2Cl]$.[31] Large hyperfine splittings were also observed for the very weakly coupled complexes [Fe(TPP)Cl],[30] [Fe(OEP)Cl],[30] and $[Fe(pyrrolidyl\text{-}dtc)_3]$.[34]

Acknowledgment. The Mössbauer spectra were obtained during a period of study leave at the University of Liverpool by P.E.C.; the hospitality of the Physics Department and useful discussions with C. D. Johnson and J. D. Rush are gratefully acknowledged. Grants from the Australian Research Grants Scheme (to K.S.M. and A.H.W.) and Monash University Special Research Grants (to K.S.M.) are gratefully acknowledged. We are grateful to Dr. P. J. Newman for providing the crystals of the iron complex and to Dr. J. R. Pilbrow for access to the ESR spectrometer.

Registry No. I, 87371-98-0.

Supplementary Material Available: Least-squares planes (Table V), non-hydrogen anisotropic thermal parameters (Table VI), atomic fractional cell and isotropic thermal parameters (hydrogen atoms) (Table VII), hydrogen atom geometries (Table VIII), structure factor amplitudes (Table IX), temperature-dependent magnetic susceptibility data (Table X), and the unit cell projected down b (Figure 7) (17 pages). Ordering information is given on any current masthead page.

(34) Rickards, R.; Johnson, C. E.; Hill, H. A. O. *J. Chem. Phys.* **1969**, *51*, 846.

Contribution from the Department of Chemistry and Biochemistry and Molecular Biology Institute, University of California, Los Angeles, California 90024

Crystal Structure and Properties of a Potassium Cryptate Salt of Bis(4-methylimidazolato)(tetraphenylporphinato)iron(III)

ROBERT QUINN, CHARLES E. STROUSE, and JOAN S. VALENTINE*

Received September 13, 1982

The synthesis and characterization of the potassium cryptate salt of bis(4-methylimidazolato)(tetraphenylporphinato)iron(III) (**1**) are reported. The salt crystallizes as the toluene solvate, $C_{77}FeH_{82}KN_{10}O_6$, in the triclinic space group $P\bar{1}$ with 2 formula units in the unit cell. At 117 K, the unit cell parameters are a = 14.63 (1) Å, b = 14.68 (1) Å, c = 17.20 (1) Å, α = 93.67 (7)°, β = 87.44 (7)°, and γ = 109.69 (7)°. The structure was solved with 3655 observed reflections, and refinement led to conventional and weighted R values of 10.7 and 10.1. The mean Fe–N(porphyrin) bond length, 1.998 (25) Å, is consistent with those of other low-spin ferric porphyrin complexes. The Fe–N(ligand) bond lengths are 1.928 (12) and 1.958 (12) Å. A comparison with Fe–N(ligand) bond lengths of $[FeTPP(ImH)_2]Cl$ (TPP = tetraphenylporphyrin; ImH = imidazole) indicates that deprotonation of imidazole may result in a 0.06-Å shortening of the axial bond lengths. Visible and EPR spectral results are consistent with the presence of a low-spin, six-coordinate ferric porphyrin complex in dimethylacetamide solution and in the solid. A comparison of the results of cyclic voltammetry of **1** and its protonated analogue, $[FeTPP(4MeImH)_2]SbF_6$ (4MeImH = 4-methylimidazole), indicates that reduction of the imidazolate complex occurs at a potential that is 700 mV more negative than that of the imidazole complex.

Introduction

Imidazolate complexes of iron porphyrins have been synthesized and studied recently[1-13] in the hope that their properties may provide information concerning the effect of deprotonation or strong hydrogen bonding of the axial histidyl imidazole ligand on the properties of certain hemoproteins. For at least one such protein, horseradish peroxidase (HRP), NMR evidence indicates that the axial histidyl imidazole is not totally deprotonated.[14] However, the possibility remains that some of the properties of HRP that are unusual when compared to hemoglobin or myoglobin,[14,15] for example, may be accounted for by a coordinated imidazole strongly hydrogen bonded to a protein residue or the protein backbone.[1] A survey of crystallographically characterized hemoproteins indicates that such hydrogen bonding is a common feature of these proteins.[16] Imidazolate is a model for the extreme case of a strongly hydrogen-bonded imidazole and thus information concerning imidazolate complexes of iron porphyrins may prove useful in understanding properties of hemoproteins in general as well as the case of any hemoprotein that may be

(1) Quinn, R.; Nappa, M.; Valentine, J. S. *J. Am. Chem. Soc.* **1982**, *104*, 2588-2595.
(2) Nappa, M.; Valentine, J. S.; Synder, P. A. *J. Am. Chem. Soc.* **1977**, *99*, 5799-5800.
(3) Landrum, J. T.; Hatano, K.; Scheidt, W. R.; Reed, C. A. *J. Am. Chem. Soc.* **1980**, *102*, 6729-6735.
(4) Landrum, J. T.; Grimmett, D.; Haller, K. J.; Scheidt, W. R.; Reed, C. A. *J. Am. Chem. Soc.* **1981**, *103*, 2640-2650.
(5) Peisach, J.; Mims, W. B. *Biochemistry* **1977**, *16*, 2795-2799.
(6) Peisach, J.; Blumberg, W. E.; Adler, A. *Ann. N.Y. Acad. Sci.* **1973**, *206*, 310-327.
(7) Cohen, I. A.; Ostfeld, D. *ACS Symp. Ser.* **1974**, *No. 5*, 221-233.
(8) Swartz, J. C.; Stanford, M. A.; Moy, J. N.; Hoffman, B. M.; Valentine, J. S. *J. Am. Chem. Soc.* **1979**, *101*, 3396-3398.
(9) Stanford, M. A.; Swartz, J. C.; Phillips, T. E.; Hoffman, B. M. *J. Am. Chem. Soc.* **1980**, *102*, 4492-4499.
(10) Stein, P.; Mitchell, M.; Spiro, T. G. *J. Am. Chem. Soc.* **1980**, *102*, 7795-7797.
(11) Mincey, T.; Traylor, T. G. *J. Am. Chem. Soc.* **1979**, *101*, 765-766.
(12) Chacko, V. P.; La Mar, G. N. *J. Am. Chem. Soc.* **1982**, *104*, 7002-7007.
(13) Stong, J. D.; Burke, J. M.; Daly, P.; Wright, P.; Spiro, T. G. *J. Am. Chem. Soc.* **1980**, *102*, 5815-5819.
(14) La Mar, G. N.; de Ropp, J. S. *Biochem. Biophys. Res. Commun.* **1979**, *90*, 36-41.
(15) Kobayashi, K.; Tamura, M.; Hayashi, K.; Hori, H.; Morimoto, H. *J. Biol. Chem.* **1980**, *255*, 2239-2242.
(16) Valentine, J. S.; Sheridan, R. P.; Allen, L. C.; Kahn, P. C. *Proc. Natl. Acad. Sci. U.S.A.* **1979**, *76*, 1009-1013.

0020-1669/83/1322-3934$01.50/0